

OPEN ACCESS

EDITED BY Sarmistha Saha, GLA University, India

REVIEWED BY

Li Li,

First Affiliated Hospital of Jilin University, China Ramtej Verma,

Gujarat University, Ahmedabad, India

*CORRESPONDENCE Lei Cao, ⊠ cl_ent@163.com

[†]These authors have contributed equally to this work

RECEIVED 07 October 2025 ACCEPTED 15 October 2025 PUBLISHED 30 October 2025

CITATION

Wu J, Sun Y, Wang S, Zhang Q, Lin Y, Liu C, Ai M, Yu F and Cao L (2025) 1-stearoyl-2-arachidonoyl-driven B Cell metabolic dysregulation in chronic rhinosinusitis with nasal polyps: insights from Mendelian randomization and single-cell RNA sequencing. *Front. Pharmacol.* 16:1719897. doi: 10.3389/fphar.2025.1719897

COPYRIGHT

© 2025 Wu, Sun, Wang, Zhang, Lin, Liu, Ai, Yu and Cao. This is an open-access article distributed under the terms of the Creative Commons Attribution License (CC BY). The use, distribution or reproduction in other forums is permitted, provided the original author(s) and the copyright owner(s) are credited and that the original publication in this journal is cited, in accordance with accepted academic practice. No use, distribution or reproduction is permitted which does not comply with these terms.

1-stearoyl-2-arachidonoyl-driven B Cell metabolic dysregulation in chronic rhinosinusitis with nasal polyps: insights from Mendelian randomization and single-cell RNA sequencing

Jian Wu^{1†}, Yifang Sun^{2†}, Shuyue Wang^{1†}, Qian Zhang³, Ying Lin¹, Caipeng Liu¹, Maomao Ai¹, Feng Yu^{1†} and Lei Cao^{1†}*

¹Department of Otorhinolaryngology-Head and Neck Surgery, Guangzhou Red Cross Hospital of Jinan University, Guangzhou, Guangdong, China, ²Department of Ophthalmology, Guangzhou Red Cross Hospital of Jinan University, Guangzhou, Guangdong, China, ³Department of Otorhinolaryngology, The Forth People's Hospital of Guiyang, Guiyang, Guizhou, China

Background: Chronic rhinosinusitis with nasal polyps (CRSwNP), an inflammatory condition of unclear etiology, may involve immune dysregulation and metabolic alterations.

Methods: Utilizing Mendelian randomization, we investigated causal links between CRSwNP and profiles of 731 immune cell types and 1,400 metabolites. Single-cell RNA sequencing (scRNA-seq) was employed for cell type identification and transcription factor analysis. Metabolic profiling characterized cellular subpopulations, while Gene Set Enrichment Analysis (GSEA) and machine learning pinpointed key genes functionally linked to immune and inflammatory pathways (categorized via WGCNA and Metascape). **Results:** We identified expression of HLA-DR on CD33- HLA-DR + B cells and the lipid metabolite 1-stearoyl-2-arachidonoyl as risk factors for CRSwNP. scRNA-seq further revealed these specific B cell subpopulations exhibit metabolic levels linked to immune responses. Bulk RNA analysis confirmed upregulation of genes CD27 and DERL3, while machine learning identified a signature of ten key genes showing positive correlation with B cell regulatory functions.

Conclusion: This integrated study advances understanding of immunemetabolic crosstalk in CRSwNP pathogenesis, highlighting the role of metabolite-influenced B cell subsets in shaping the immune microenvironment, thereby suggesting novel therapeutic targets.

KEYWORDS

CRSwNP, B-cell, metabolism, immunity, Mendelian randomization, single-cell RNA sequencing

1 Introduction

CRSwNP is a persistent inflammatory disorder affecting the nasal mucosa and paranasal sinuses. Characterized by infiltration of diverse inflammatory cells, this condition typically presents with symptoms including persistent nasal congestion, rhinorrhea, pain, and hyposmia/anosmia (Bachert et al., 2021). Studies have shown that

the prevalence of CRSwNP is about 1.1% in the United States and 2.1%–4.4% in Europe (Laidlaw et al., 2021). Notably, CRSwNP affects about 20%–30% of patients with chronic rhinosinusitis (CRS), which imposing a substantial socioeconomic burden and significantly impairing patients' quality of life. Current treatment for CRSwNP mainly includes corticosteroid drugs and endoscopic sinus surgery; however, these approaches are associated with potential adverse effects (e.g., from corticosteroids) and notably high recurrence rates following surgery (Hox et al., 2020).

While the precise etiology of CRSwNP remains incompletely elucidated, the roles of immune dysregulation and metabolic perturbations in its pathogenesis have garnered increasing attention (Veloso-Teles et al., 2019). Emerging evidence suggests metabolites can modulate immune cell function (Veloso-Teles et al., 2019). CRSwNP is commonly stratified into eosinophilic (ECRSwNP) and non-eosinophilic (non-ECRSwNP) subtypes based on tissue eosinophilia levels (Cao et al., 2009). Notably, linoleic acid has been implicated in eCRSwNP pathogenesis through its suppressive effects on eosinophilic inflammation (Ma et al., 2021). Furthermore, M2 macrophages contribute to CRSwNP development via complex immune responses and tissue remodeling processes, with several M2associated hub genes identified as critical contributors (Zhu et al., 2022). Interestingly, resolvin D1 (RvD1), a specialized pro-resolving mediator, promotes macrophage polarization towards this M2 phenotype (Vickery et al., 2021). B-cell responses, including proliferation, antibody production, and aberrant pathway activation, are increasingly recognized as key drivers in CRSwNP (Bai and Tan, 2023), and heightened expression of B-cell activating factor (BAFF) is strongly linked to postoperative recurrence (Zhang et al., 2022). Intriguingly, RvD1 and its precursor 17-HDHA have been shown to influence naïve B-cell differentiation (Kim et al., 2015). Collectively, these findings underscore the intricate interplay between immunity and metabolism in CRSwNP. This relationship is further highlighted by distinct metabolic profiles observed across CRSwNP subtypes. Specific metabolites, including maresins, specialized pro-resolving lipid mediators (SPMs), and linoleic acid, are considered potential diagnostic biomarkers (Guo et al., 2023), while enzymes and metabolites involved in fatty acid metabolism represent promising therapeutic targets (Miyata et al., 2019). Nevertheless, a comprehensive understanding of the specific metabolic-immunoregulatory mechanisms governing pathogenesis is still lacking.

In this study, we employed an integrated approach utilizing Mendelian randomization, single-cell RNA sequencing (scRNA-seq), and transcriptome analysis to elucidate the underlying immunometabolic regulatory mechanisms in CRSwNP. Specifically, Mendelian randomization was applied to identify metabolites and immune cells exhibiting causal relationships with CRSwNP. Subsequently, integrated scRNA-seq and transcriptomic analyses were leveraged to delineate the specific immunomodulatory roles of key metabolites within the CRSwNP context.

Abbreviations: CRS, chronic rhinosinusitis; CRSwNP, Chronic rhinosinusitis with nasal polyps; ECRSwNP, eosinophilic Chronic rhinosinusitis with nasal polyps; non-ECRSwNP, non-eosinophilic chronic rhinosinusitis with nasal polyps; RVD1, resolvin D1; SPM, specialised pro-resolving lipid mediators; IVW, inverse variance weighting; AUC, Area Under Curve; Km, K-means; RFE, Recursive Feature Elimination; BAFF, B cell-activating factor of the TNF family; TNFR, tumor necrosis factor receptor.

2 Methods

2.1 Mendelian randomization analysis

Mendelian randomization (MR) utilizes genetic variants as instrumental variables, adhering to the principle of Mendelian inheritance, to infer causal relationships between exposures and outcomes while mitigating confounding biases. In this study, we employed a two-sample MR design to investigate the causal effects of plasma metabolites and circulating immune cells on CRSwNP (Zhu et al., 2018). The results of which Mendelian randomization satisfy three core assumptions: (1) Association assumption: The instrumental variables (IVs) must be strongly associated with the exposure. (2) Independence assumption: The IVs must be independent of confounding factors that influence the exposureoutcome relationship. (3) Exclusion restriction assumption: The IVs must influence the outcome solely through the exposure pathway. Primary MR analyses were conducted using the inverse variance weighted (IVW) method implemented in the TwoSampleMR package. We defined plasma metabolites and peripheral blood immune cell phenotypes as exposures, and CRSwNP as the outcome. Exposure data for 1,400 plasma metabolites were sourced from the genome-wide association study (GWAS) by Chen et al. (2023). Exposure data for 731 circulating immune cell phenotypes, encompassing diverse developmental stages and cell types, were obtained from a comprehensive GWAS of peripheral blood immune cells (Orru et al., 2020). This dataset included absolute cell counts, relative cell counts, median fluorescence intensity (MFI) reflecting surface antigen expression, and morphological parameters. We performed MR analyses to identify metabolites and immune cell traits causally associated with CRSwNP risk. All reported associations underwent false discovery rate (FDR) correction for multiple testing. Ethical approval and participant informed consent were secured in the original studies providing the GWAS summary statistics used in this MR analysis. These data are publicly accessible via the GWAS catalog (https://www.ebi.ac.uk/gwas/) under the accession codes provided in the respective publications (Burgess et al., 2013).

2.2 Metabolomic profiling of CRSwNP

Nasal secretion samples were collected from 12 healthy individuals and 19 patients with CRSwNP. These samples were prospectively collected specifically for this study at Guangzhou Red Cross Hospital. This study was approved by the Medical Ethics Committee of Guangzhou Red Cross Hospital (Approval No: 2024-128-01), conducted in accordance with the Declaration of Helsinki, and all participants provided written informed consent. Clinical trial number: not applicable. Following nasal mucosa preparation using ephedrine and 2% tetracaine, sterile swabs were employed to gather secretions from the middle meatus, and these samples were subsequently stored at -80 °C. For metabolite extraction, 100 µL of each sample was combined with 700 µL of extraction solvent (methanol:acetonitrile:water = 4:2:1, v/v/v), vortexed, incubated at -20 °C for 2 h, and centrifuged at 25,000 × g for 15 min at 4 °C; the resulting supernatant was then evaporated and reconstituted in 180 µL of methanol:water (1:1, v/v). Liquid

chromatography-mass spectrometry (LC-MS) analysis was conducted using a Thermo Q Exactive system equipped with a BEH C18 column, utilizing specific mobile phases for positive and negative ion modes and electrospray ionization (ESI) in full scan mode (m/z 70–1,050). Metabolites were identified by referencing the BGI HR-PMDB and mzCloud databases, and differential metabolites between the CRSwNP and normal groups were determined through principal component analysis (PCA), partial least squares discriminant analysis (PLSDA), and orthogonal partial least squares discriminant analysis (OPLSDA). Finally, pathway enrichment analysis was performed using the Kyoto Encyclopedia of Genes and Genomes (KEGG) database.

2.3 Single-cell RNA sequencing data processing

Guided by Mendelian randomization findings identifying metabolites and immune cells potentially causally linked to CRSwNP, we performed integrated analyses using scRNA-seq data. Single-cell transcriptomic data from CRSwNP patient samples were retrieved from the Gene Expression Omnibus (GEO) database under accession number GSE196169 (Bangert et al., 2022). Raw scRNA-seq data processing, quality control, normalization, dimensionality reduction, clustering, annotation were conducted using the Seurat package (v4.3.0) (Zheng et al., 2017). Quality control filtering was applied as follows: cells expressing fewer than 200 genes or more than 4,000 genes were excluded, and cells with mitochondrial gene content exceeding 10% were also removed. Normalization and feature selection: Filtered gene expression counts were normalized using the NormalizeData function. Subsequently, variable genes (HVGs) were identified FindVariableFeatures. Scaling, dimensionality reduction, and integration: Expression data were scaled (ScaleData) and centered prior to principal component analysis (PCA). To mitigate technical batch effects, batch correction was performed using the RunHarmony function (Stuart et al., 2019). The resulting integrated data were then subjected to uniform manifold approximation and projection (UMAP) for non-linear dimensionality reduction and visualization. Cell clustering and annotation: Cells were clustered using the shared nearest neighbor (SNN) modularity optimization approach (FindNeighbors followed by FindClusters) based on a selected number of principal components. Cell types were annotated using the SingleR package (Kanehisa et al., 2023) with reference datasets. Metabolic pathway scoring and differential expression analysis: Metabolic pathway activity was inferred and scored per cell using gene signatures derived from KEGG pathways. Finally, the FindMarkers function was employed to identify differentially expressed genes (DEGs) between biologically relevant subpopulations.

2.4 Bulk RNA-seq data processing

To validate immunometabolic regulatory genes identified through scRNA-seq analysis in CRSwNP, we performed

integrative transcriptomic analysis using bulk RNA-seq datasets. Datasets GSE36830 and GSE23552 were retrieved from the GEO database (Stevens et al., 2015; Plager et al., 2010). The results after batch removal were visualized by the principal component analysis method to finally obtain a comprehensive data expression matrix, from which differential genes obtained from a single-cell analysis were extracted for subsequent analysis and modeling. GSVA was used for enrichment analysis, limma package was used for differential analysis, volcano plots obtained significant differentially expressed genes, and correlation analysis was used to explore the correlation changes of genes (Ritchie et al., 2015).

2.5 Gene set enrichment analyses

GSEA analysis assesses the distribution trend of genes in gene expression for a predefined gene set (Powers et al., 2018). GOBP_B_ CELL_RECEPTOR_SIGNALING_PATHWAY was selected as a predefined gene set to evaluate the expression of B-cell receptor signaling pathways in differential genes and significant signaling pathways were selected by FDR q-value<0.25. Ssgsea allows for assessment of the enrichment of a gene set in a single sample (Jin et al., 2021). Immune infiltration analysis was performed by ssgsea. And the expression of genes in B cells was analyzed.

2.6 Single-cell transcription factor and cell communication analysis

Transcription Factor (TF) Analysis: B cell subsets isolated from scRNA-seq data were subjected to TF activity inference using the DoRothEA regulon database (Xu et al., 2024) via the run_viper function. Data scaling ensured comparability across cells. TF activity scores were computed using GetAssayData, with the top 20 most variable TFs visualized in heatmaps generated by the pheatmap package (minsize parameter = 4). Cell-Cell Communication Analysis: Intercellular signaling was investigated using CellCall (Zhang et al., 2021). Cellular populations were categorized as B cells and non-B cells. The analysis workflow included: (1) Object creation with CreateNichConObject; (2) Pathway-centric communication network identification via TransCommuProfile; (3) Statistical filtering (padj <0.05) and correlation analysis of significant ligand-receptor pairs.

2.7 Machine learning

We applied machine learning for feature selection and predictive modeling using the randomForest package (Ishwaran and Kogalur, 2010). Models were trained on the integrated bulk RNA-seq data from GSE36830 and GSE23552, with internal validation via 5-fold cross-validation and bootstrap resampling. This robust method efficiently handles high-dimensional data while maintaining noise resistance. Key genes were identified via feature importance ranking, followed by multivariable logistic regression modeling (glm function). Models underwent bootstrap validation (1,000 iterations) with performance quantification via sensitivity/ specificity and receiver operating characteristic (ROC) curves (roc

function), including AUC calculations. Decision curve analysis (decision_curve function) evaluated clinical utility, while nomogram visualization utilized the regplot package.

2.8 Immune infiltration analysis

Immune microenvironment profiling was conducted via the IOBR package (Newman et al., 2015), employing CIBERSORT (deconvo_cibersort) for relative immune cell quantification and MCP-counter for absolute cell abundance assessment. Analysis was restricted to DEGs meeting thresholds (adj. p < 0.05, $|\log 2FC| > 0.5$). Spearman correlations (psych:corr.test) with FDR correction analyzed gene-infiltration relationships, with identical methodology applied to inflammatory factors.

2.9 Clustering and Co-expression analysis

Consensus clustering (ConsensusClusterPlus) (Wilkerson and Hayes, 2010) defined molecular subtypes using k-means clustering (kmax = 10, 100 iterations, 80% sample retention). Cluster stability was evaluated via consensus matrices and item-consistency indices (calcICL). Weighted gene co-expression network analysis (WGCNA) (Langfelder and Horvath, 2008) identified coregulated modules through: 1) Selection of top 2000 variant genes (goodSamplesGenes QC), 2) Sample outlier removal (hclust + cutreeStatic), 3) Soft-threshold determination (pickSoftThreshold), 4) Network construction

(blockwiseModules), 5) Module eigengene extraction (moduleEigengenes), and 6) Module-trait correlation (cor + corPvalueStudent). Significant modules (p < 0.05) underwent functional annotation in Metascape (Zhou et al., 2019).

2.10 Statistical analysis

All analyses used R v4.2.3. Statistical methods included: Spearman correlation with FDR correction (psych:corr.test), data scaling (scaleData), recursive feature elimination with 5-fold cross-validation (rfe), group comparisons via Wilcoxon test, odds ratio calculation with forest plotting (forestploter), and Benjamini-Hochberg FDR adjustment. Significance was defined as two-sided p < 0.05 unless specified.

3 Results

3.1 Mendelian randomization analysis of immune cells and metabolites

Mendelian randomization analysis was performed to assess causal relationships between CRSwNP and 731 immune cell phenotypes or 1,400 plasma metabolites. Analysis of immune cells revealed that HLA-DR expression on CD33⁻ HLA-DR⁺ B cells exhibited a potential causal association with CRSwNP risk (beta = 0.181, FDR = 0.007; Figures 1A-D). For metabolites, 1-stearoyl-2-arachidonoyl showed evidence of significant causal

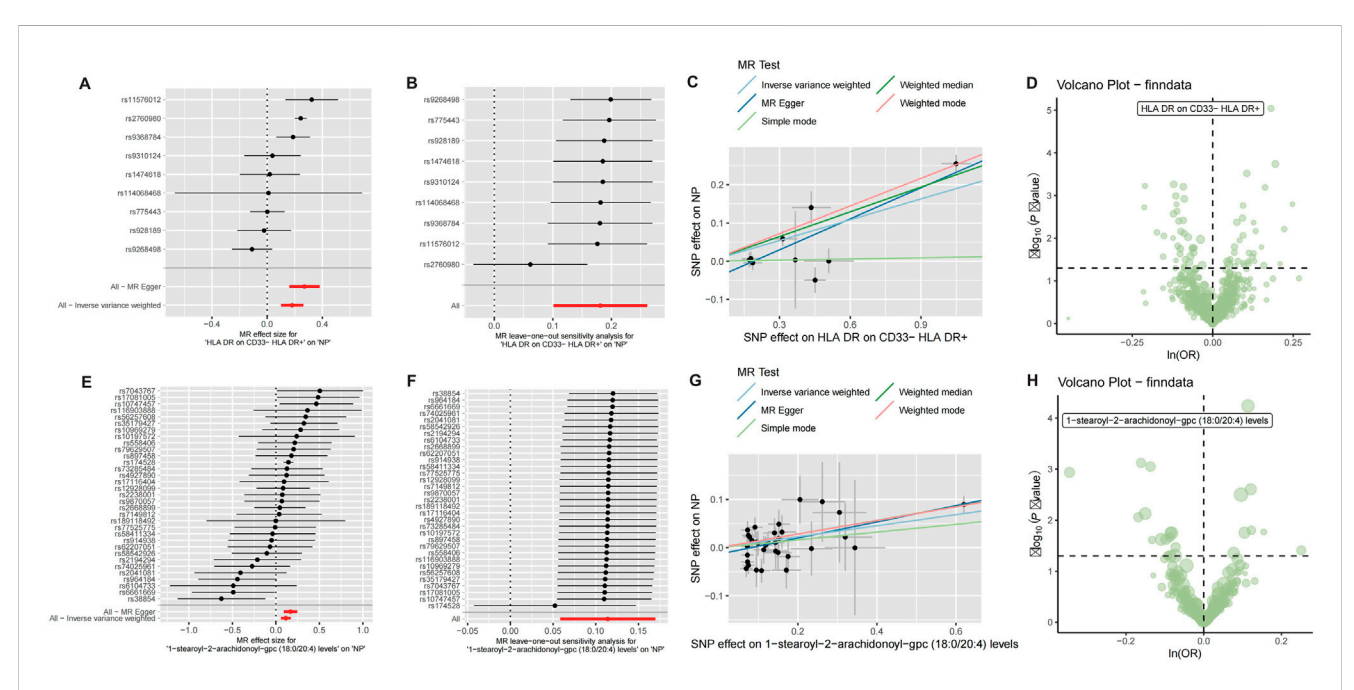


FIGURE 1
Mendelian randomization analysis of CRSwNP with immune cells and metabolites. (A) Forest plot of Mendelian randomization results for CRSwNP and HLA DR on CD33- HLA DR+. (C) Scatter plot of Mendelian randomization for CRSwNP and HLA DR on CD33- HLA DR+. (D) Volcano plot of Mendelian randomization for CRSwNP and immune cells. (E) Forest plot of Mendelian randomization results for CRSwNP and 1-stearoyl-2-arachidonoyl-gpc. (F) Leave-out analysis for CRSwNP and 1-stearoyl-2-arachidonoyl-gpc. (G) Scatter plot of Mendelian randomization for CRSwNP and 1-stearoyl-2-arachidonoyl-gpc. (H) Volcano plot of Mendelian randomization results for CRSwNP and metabolites.

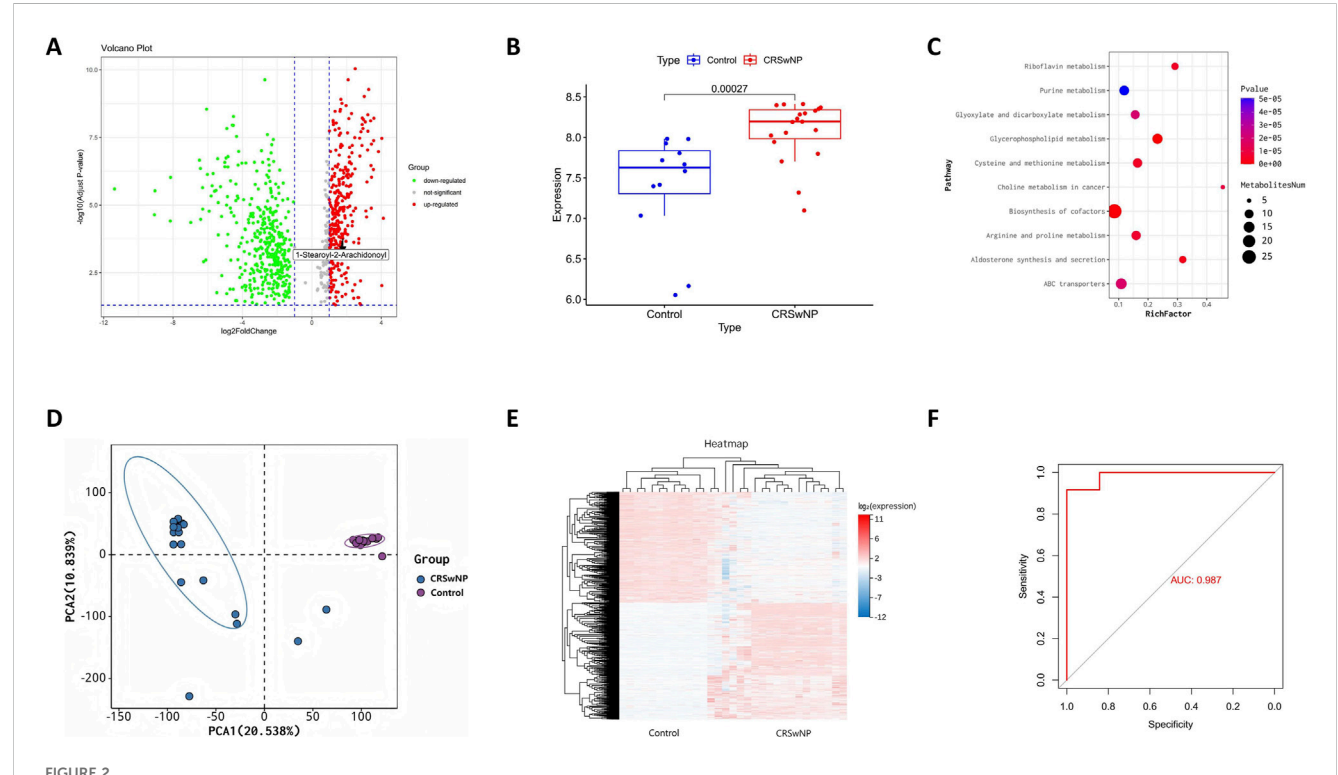
effects on CRSwNP development (beta = 0.114, FDR = 0.015; Figures 1E–H). Complete MR results are documented in Supplementary Table S1, S2.

3.2 Integrated metabolomic profiling of CRSwNP

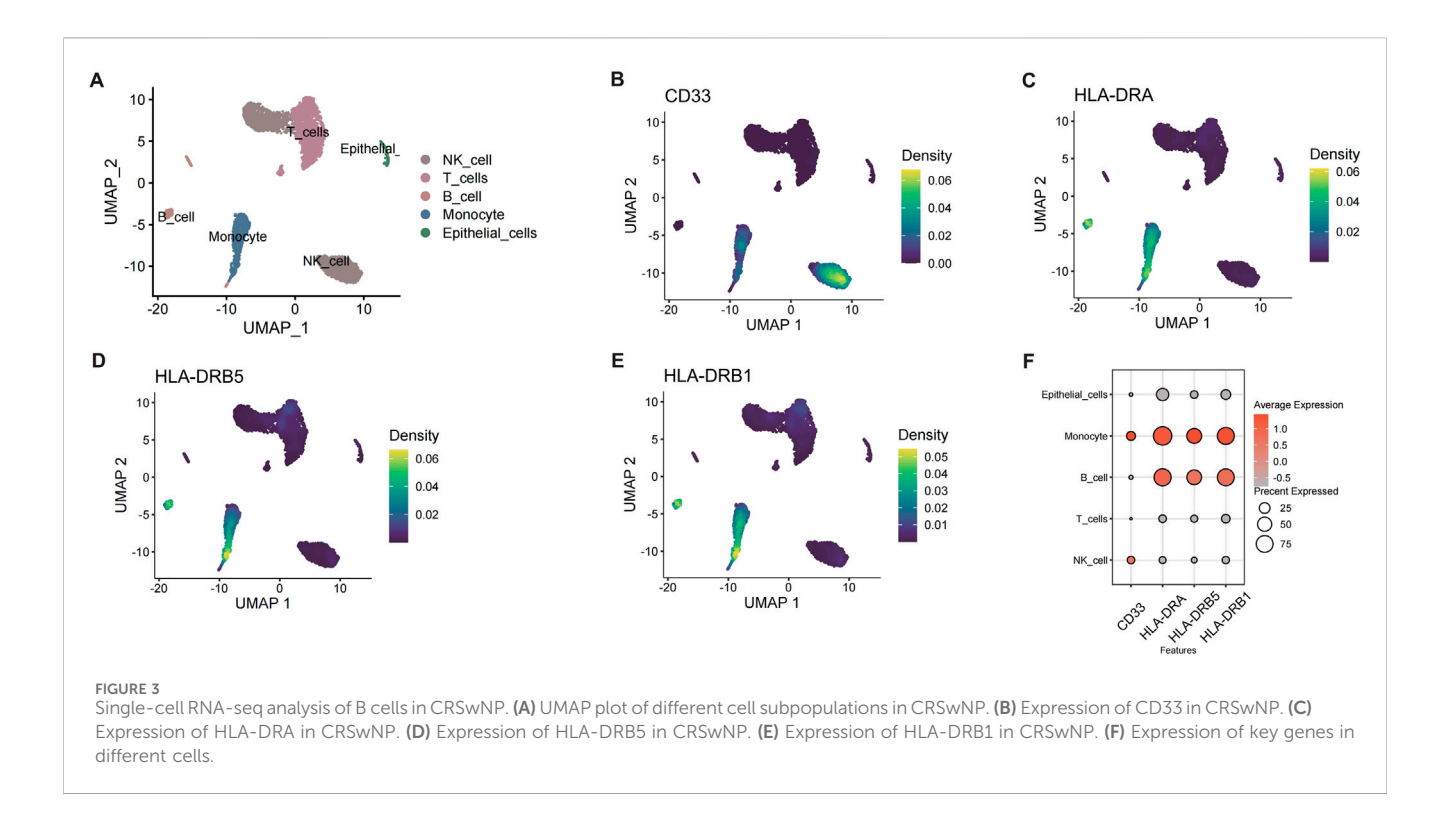
To further elucidate the metabolic alterations linked to CRSwNP, particularly the role of 1-stearoyl-2-arachidonoyl identified through Mendelian randomization, we performed metabolomic profiling comparing CRSwNP and healthy controls which were prospectively collected specifically for this study at Guangzhou Red Cross Hospital. Volcano plot analysis revealed significant upregulation of 1-stearoyl-2-arachidonoyl in CRSwNP (Figure 2A), confirmed by elevated levels in boxplot visualization (Figure 2B). **KEGG** pathway enrichment identified glycerophospholipid metabolism and cysteine-methionine metabolism as significantly dysregulated pathways (Figure 2C), consistent with 1-stearoyl-2-arachidonoyl's role as a key glycerophospholipid. 1-stearoyl-2-arachidonoyl is a diacylglycerol species within the glycerophospholipid pathway, serving as a precursor for arachidonic acid release and subsequent eicosanoid production, which are known to modulate inflammatory responses in mucosal tissues. Principal component analysis (PCA) demonstrated clear separation between groups (Figure 2D), indicating distinct metabolic signatures. Hierarchical clustering of metabolites further corroborated disease-associated patterns (Figure 2E). Receiver operating characteristic (ROC) analysis revealed exceptional diagnostic performance for 1-stearoyl-2-arachidonoyl (AUC = 0.987, Figure 2F), supporting its biomarker potential. These results establish glycerophospholipid metabolic dysregulation as a hallmark of CRSwNP, highlighting 1-stearoyl-2-arachidonoyl's central role.

3.3 Single-cell profiling and B Cell heterogeneity in CRSwNP

Single-cell RNA sequencing (scRNA-seq) of CRSwNP samples (GSE196169) was performed to elucidate the roles of HLA-DR+CD33- B cells and 1-stearoyl-2-arachidonoyl. After quality control and normalization, cell clustering identified five major populations: NK cells, T cells, B cells, monocytes, and epithelial cells (Figure 3A). Expression patterns of MR-implicated genes (CD33, HLA-DRA, HLA-DRB5, HLA-DRB1) were visualized across cell types (Figures 3B-E), confirming enrichment in the B cell compartment. Based on MR results for 1-stearoyl-2arachidonoyl, we computed metabolic activity scores for glycerophospholipid pathway genes (LCAT, PLA2G4, PLA2G6, PLA2G16, PLB1, TGL4, DAGD, LCAT3) within B cells. Unsupervised clustering stratified B cells into two distinct subpopulations: PC_high_B_cell (elevated phospholipid metabolism) and PC_low_B_cell (Figure 3F).



Integrated Metabolomic Profiling Identifies Dysregulated Glycerophospholipid Metabolism in CRSwNP. (A) Volcano plot displaying differential metabolites in CRSwNP versus Normal. (B) Elevated levels of 1-stearoyl-2-arachidonoyl in CRSwNP versus Normal groups. (C) KEGG pathway enrichment of differential metabolites. (D) PCA score plot demonstrating separation between CRSwNP and Normal groups based on metabolomic profiles. (E) Metabolic heatmap analysis of CRSwNP vs. Normal. (F) ROC curve analysis of 1-stearoyl-2-arachidonoyl for distinguishing CRSwNP.



3.4 Characterization of PC_high_B_cell-Associated pathways and interactions

Differential gene analysis of B cell subpopulations (PC_high_B_ cell vs. PC_low_B_cell) revealed enrichment in immune response pathways via GSEA, including adaptive immunity and immune system activation (Figure 4A). Specifically, upregulated B-cell receptor signaling pathways suggested potential metabolitereceptor interactions modulating B cell function (Figure 4B). Transcription factor profiling identified elevated activity of ATF6, SP1, IRF4, ZNF263, CREB3, and HIF1A in PC_high_B_cells (Figure 4C). Intercellular communication analysis demonstrated interactions between PC_high_B_cells preferential monocytes/epithelial cells, with signaling enriched in ErbB and chemokine pathways (Figure 4D). This was corroborated by upregulation of chemokines CCL3 CCL4 alongside enhanced antibody production in PC_high_B_ cells (Figures 4E,F), indicating metabolite-dependent B cell activation contributes to CRSwNP pathogenesis.

3.5 Bulk RNA-seq analysis of CRSwNP differential genes

While MR highlighted HLA-DR and CD33 as surface markers on B cells, scRNA-seq and bulk RNA analyses revealed downstream effectors such as CD27, DERL3, and TNFRSF17, which are functionally linked to B cell activation and survival in the context of elevated glycerophospholipid metabolism. Building on the single-cell findings, we analyzed bulk RNA-seq datasets (GSE36830 and GSE23552) to validate differentially expressed genes. After batch effect correction (Supplementary Figure S1A,B), differential

expression analysis using limma identified significant alterations: NUCB2 was downregulated while CD27 and DERL3 were upregulated in CRSwNP (Supplementary Figure S1C-E). Correlation analysis revealed co-expression patterns among key genes (Supplementary Figure S2A-C), with pairwise comparisons confirming positive correlations between DERL3-CD27 and FKBP11-CD27 (Supplementary Figure S2D,E). These findings demonstrate coordinated upregulation of CD27 and DERL3 in CRSwNP, suggesting their potential role in disease pathogenesis. These DEGs align with MR-identified B cell subsets and metabolite dysregulation, supporting the hypothesis that 1stearoyl-2-arachidonoyl drives B cell-mediated inflammation via genes involved activation (CD27) in and stress responses (DERL3).

3.6 Machine learning model for CRSwNP diagnosis

In order to further validate gene signatures, we developed a diagnostic model using random forest to identify key discriminative features. Feature importance ranking by Mean Decrease Gini identified 10 pivotal genes, including NUCB2 and CD27 (Figure 5A). Multivariable logistic regression modeling with these genes demonstrated high discriminative capacity (AUC = 0.969; Figures 5B,C), validated through bootstrap resampling with sensitivity/specificity quantification (Figures 5D–F). A nomogram visualizing predictor contributions (100 resamples, total score threshold = 0.131) and calibration curve (minimal deviation from ideal 45° line; Figure 6A) confirmed model robustness. Decision curve analysis comparing three gene-set models further established clinical utility (Figure 6B).

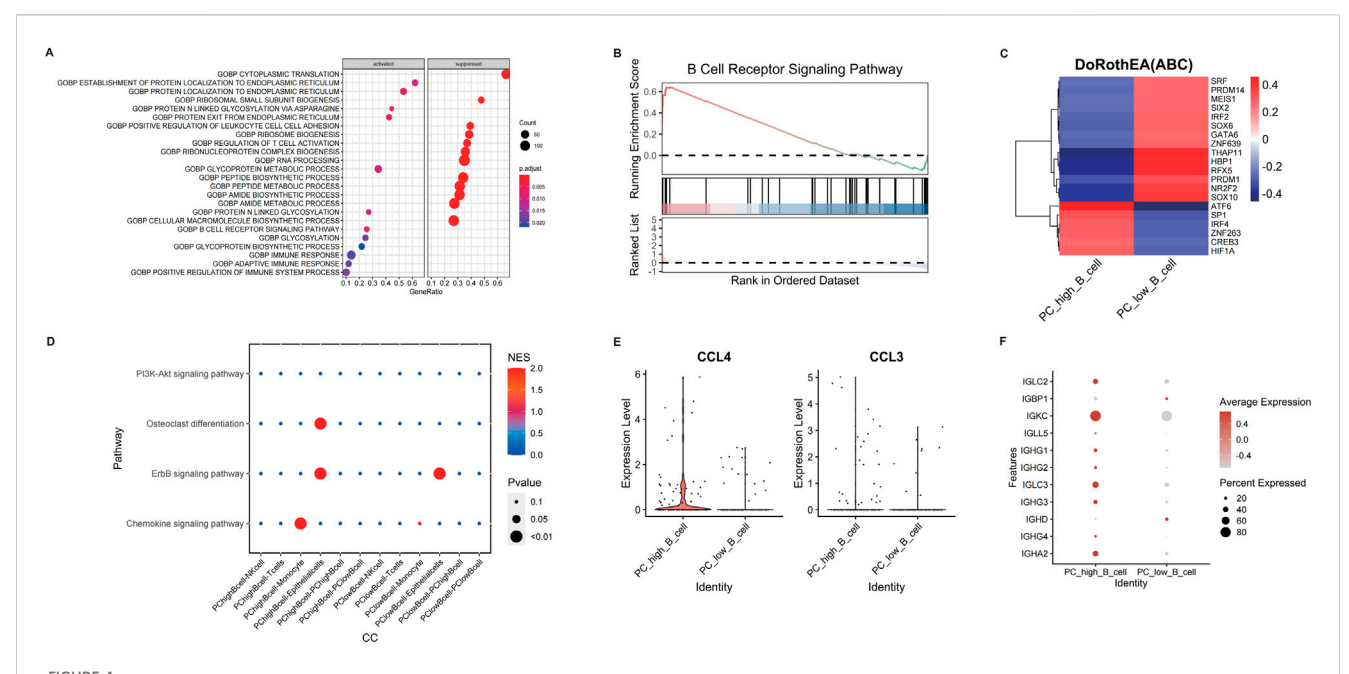


FIGURE 4
Differential analysis of different B cell subpopulations in CRSwNP. (A) GSEA enrichment analysis of differentially expressed genes in B cell subpopulations. (B) Analysis of B cell receptor pathway expression. (C) Transcription factor analysis of B cell subpopulations. (D) Cell-cell communication analysis of different cell subpopulations using CellCall. (E) Expression of CCL4 and CCL3 in different B cell subpopulations. (F) Expression of immunoglobulin-related genes in different B cell subpopulations.

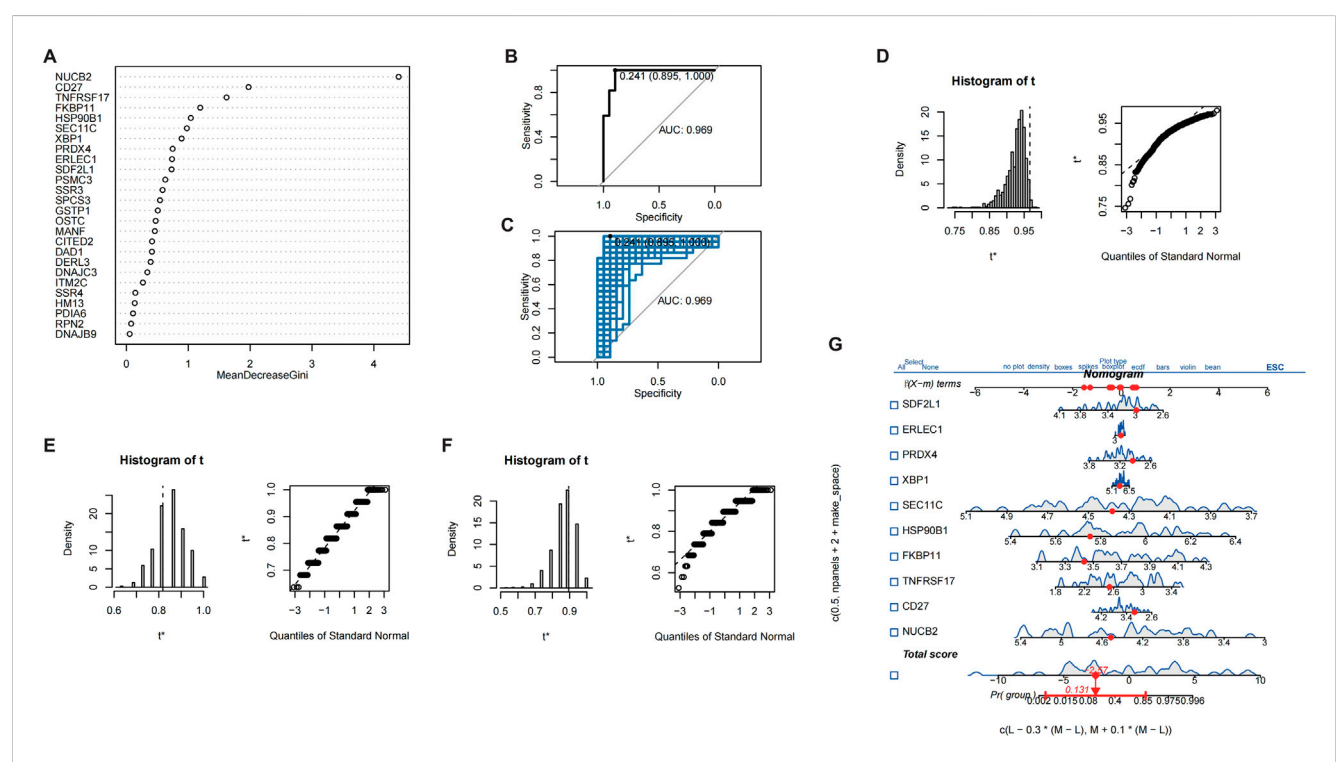
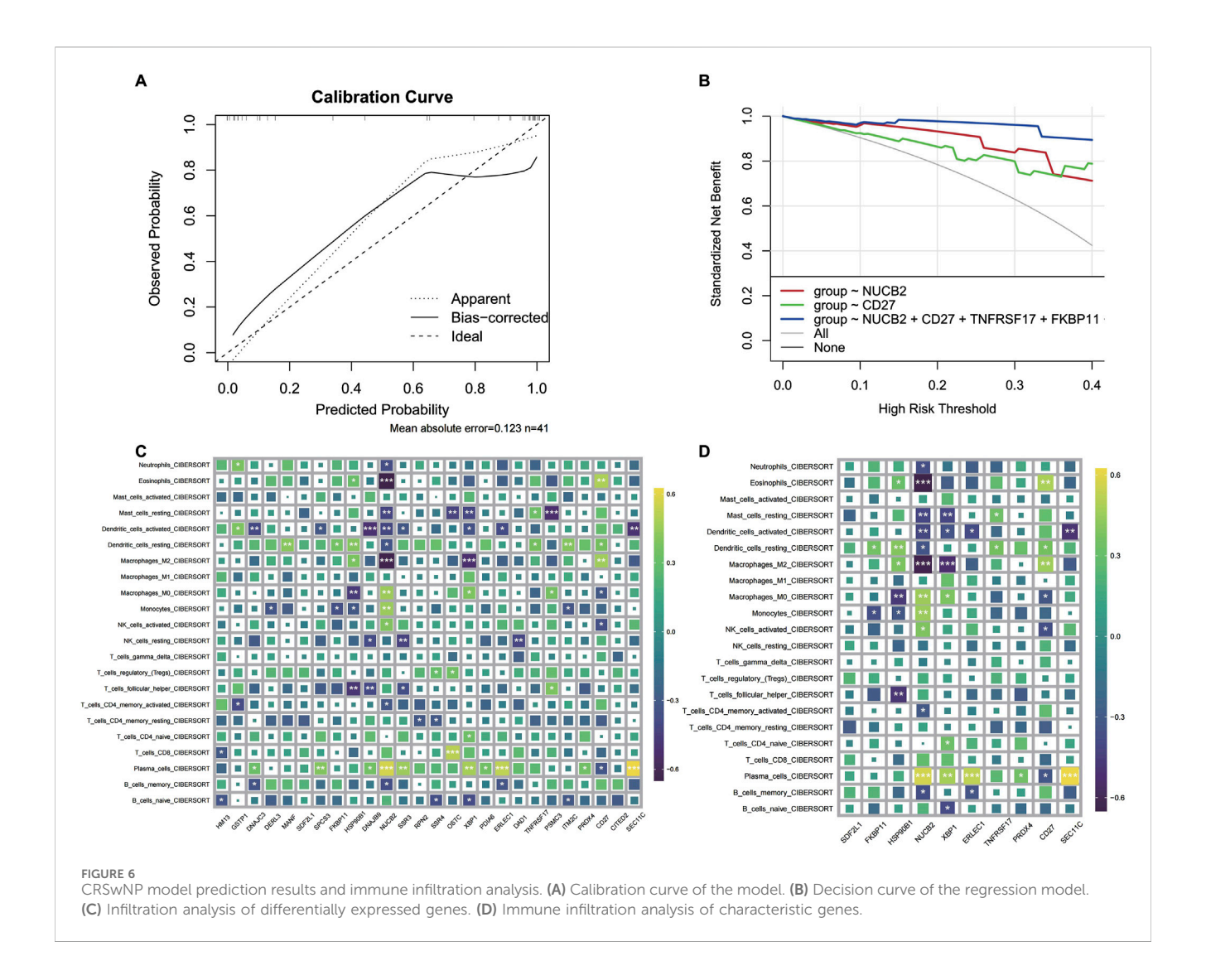


FIGURE 5
Screening of characteristic genes in CRSwNP. (A) Machine learning-based screening of characteristic genes in CRSwNP. (B) ROC curve of the results from multiple logistic regression. (C) Bootstrap validation combined with ROC. (D) Display of model bootstrap results. (E) Model sensitivity results. (F) Model specificity results. (G) Nomogram of different characteristic genes.



3.7 Immune microenvironment characterization via key gene signatures

To delineate the immunomodulatory role of identified key genes, we performed comprehensive immune infiltration analysis using CIBERSORT and ssGSEA (Figures 6C,D). Quantitative assessment via MCP-counter revealed distinct immune cell abundance patterns associated with CD27, DERL3, and TNFRSF17 expression (Figures 7A,B). Inflammatory factor profiling demonstrated significant correlations between CD27 and Th2 cytokines (IL13, IL4; Figure 7C), while B lineage-specific analysis showed positive associations of CD27, DERL3, and TNFRSF17 with B cell infiltration (Figures 7D,E). These findings suggest coordinated regulation of PC_high_B_cell functionality through metabolic-immunological crosstalk.

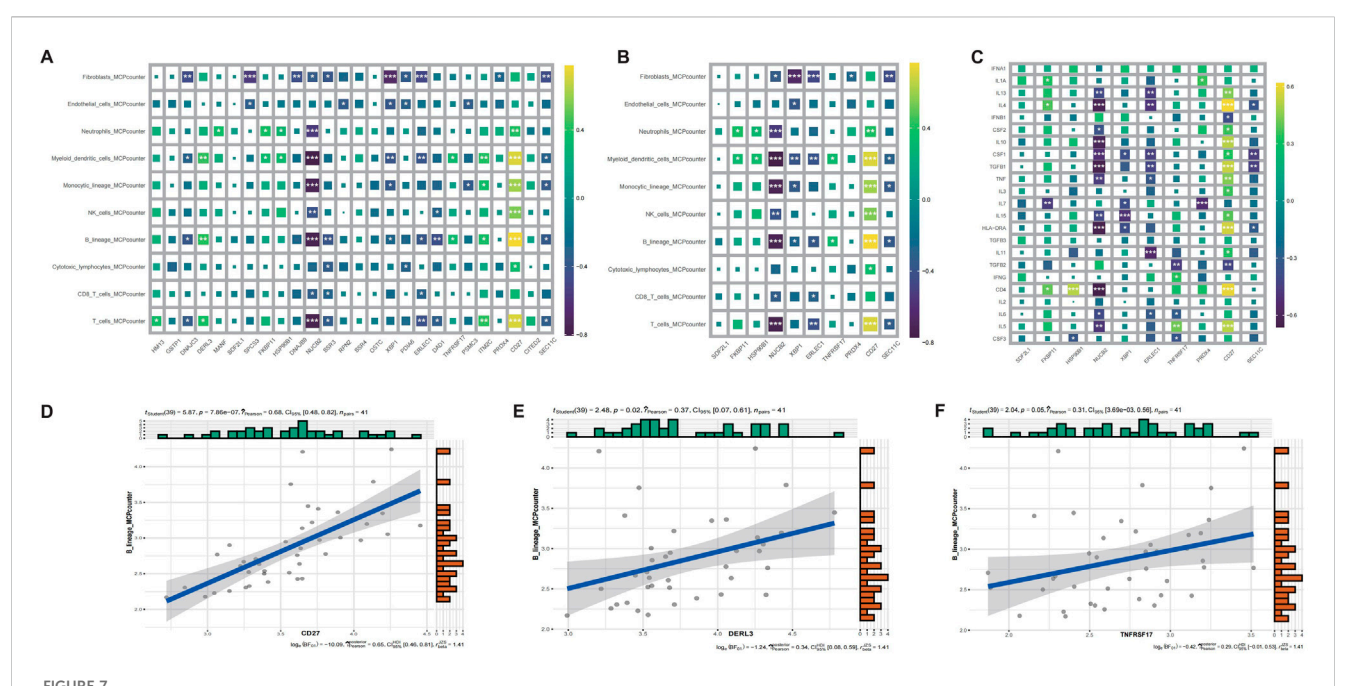
3.8 Molecular subtyping and Co-expression network analysis

To define molecular subtypes associated with CRSwNP pathogenesis, consensus clustering identified two stable

subgroups (k = 2) using k-means algorithm (100 iterations, kmax = 10). Cluster 1 exhibited elevated expression of key genes, while Cluster 2 showed reduced expression (Figures 8A,B). Inflammatory factor clustering further revealed differential abundance of CD4, IL7, and IFNA1 between subtypes (Figure 8C). Weighted gene co-expression network analysis (WGCNA) identified functionally cohesive modules, with soft-thresholding power set to 5 based on scale-free topology criteria (Figure 8D). The green module demonstrated highest immune relevance (Figure 8E), with Metascape enrichment confirming involvement in pro-inflammatory responses and cytotoxic regulation (Figure 8F; Supplementary Table S3).

4 Discussion

CRSwNP constitutes a persistent inflammatory disorder distinguished by mucosal hyperplasia and polyp formation within the sinonasal cavity, frequently characterized by chronicity, elevated recurrence rates, and heterogeneous responses to treatment (Nakayama and Haruna, 2023). These clinical complexities arise from sustained inflammation that precipitates pathological



MCPcounter immune infiltration and correlation analysis of CRSwNP genes. (A) MCPcounter quantitative infiltration analysis of differentially expressed genes. (B) MCPcounter quantitative infiltration analysis of characteristic genes. (C) Inflammatory factor infiltration analysis of characteristic genes. (D) Correlation analysis between CD27 and B cell expression. (E) Correlation analysis between DERL3 and B cell expression. (F) Correlation analysis between TNFRSF17 and B cell expression.

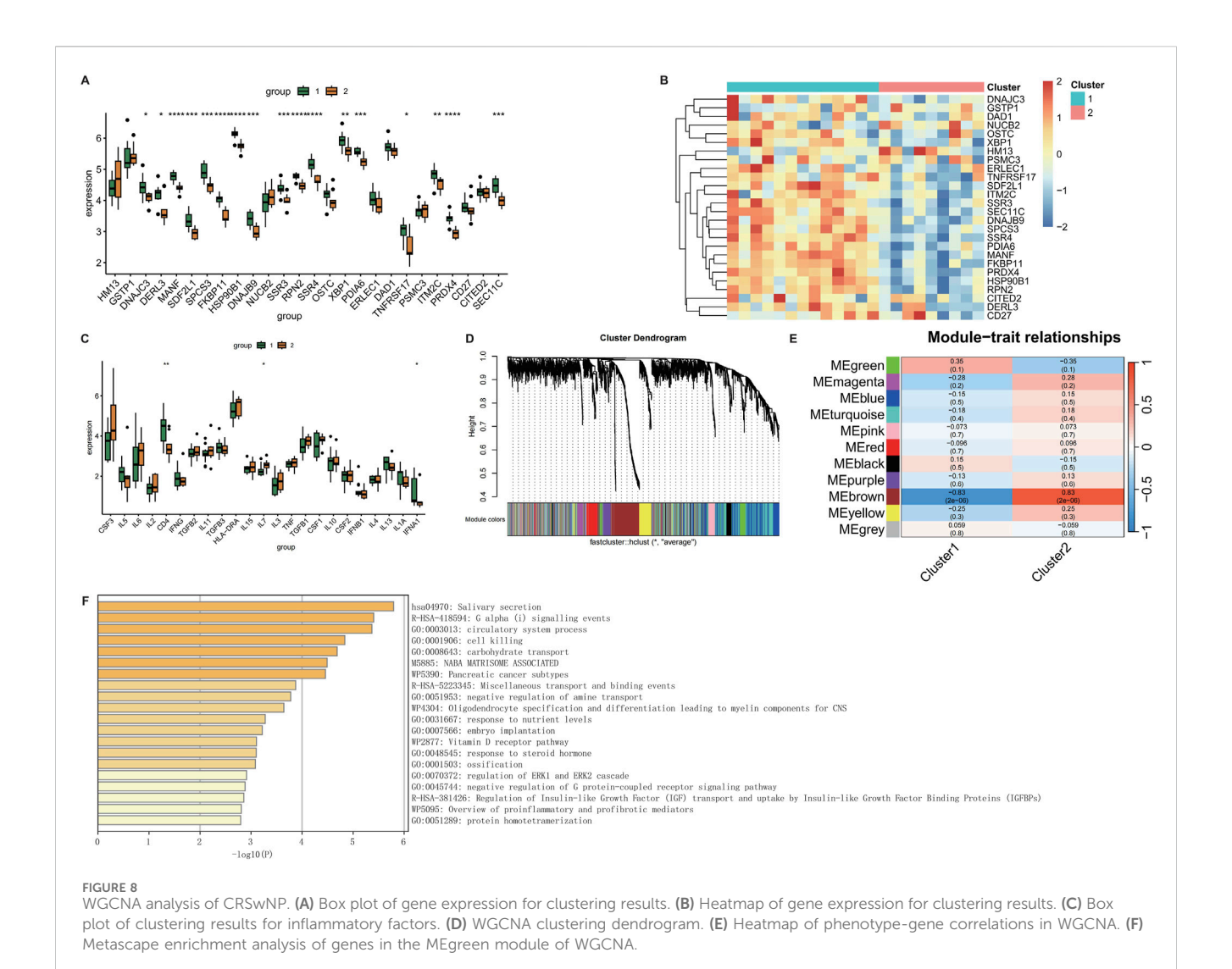
remodeling, thereby perpetuating symptom burden and rendering therapeutic management challenging. Through an integrated multiomics approach—incorporating Mendelian randomization, single-cell transcriptomics, and bulk RNA sequencing—we have elucidated dysregulated immunometabolic pathways fundamental to the pathogenesis of CRSwNP. Specifically, our investigation delineates causal contributions of HLA-DR+CD33—B cell subsets and the glycerophospholipid metabolite 1-stearoyl-2-arachidonoyl, thereby unveiling novel mechanistic associations between metabolic reprogramming and immune dysregulation in this refractory condition.

The etiology of CRSwNP is multifaceted, involving factors such as infection, allergy, environmental pollution, and anatomical abnormalities. The role of immunity in its pathogenesis has increasingly come under scrutiny (Schleimer, 2017). SResearch by Shigeharu Fujieda et al. indicates that the activation of eosinophilassociated functions may contribute to the development of nasal polyps (Fujieda et al., 2019), while Jacob G. Eide et al. identified elevated levels of functionally active antiphospholipid antibodies in CRSwNP (Eide et al., 2022). Additionally, Kathryn E. Hulse et al. demonstrated that nasal polyp tissue creates an environment conducive to B cell survival and functionality, thereby facilitating disease progression (Hulse et al., 2013). To further elucidate the immunological mechanisms driving CRSwNP, we utilized Mendelian randomization and single-cell analysis to explore the causal links between immune cells and the condition. Our findings highlight the critical role of B cells in CRSwNP, confirming their contribution to disease advancement.

As key players in the adaptive immune response, B cells not only produce antibodies and cytokines that exacerbate CRSwNP

pathogenesis but also participate in inflammation as antigenpresenting or regulatory cells (Tan et al., 2018). These cells secrete an array of cytokines, including IL-4, IL-5, IL-13, and chemokines, which amplify the inflammatory response and promote granulocyte activation and aggregation. This aligns with findings by Gwanghui Ryu, who noted that B-cell activators drive the progression of refractory CRSwNP through Th17-mediated immune responses and neutrophil recruitment (Ryu et al., 2019). Moreover, B cells serve as antigen-presenting cells, delivering antigens to T cells and triggering adaptive immune responses that result in further inflammatory cell infiltration. The chronic airway inflammation characteristic of CRSwNP fosters a unique milieu that supports B cell activation and antibody production (Feldman et al., 2017). Concurrently, activated mast cells in CRSwNP can stimulate B cells to produce IgE, intensifying the inflammatory cascade (Zhai et al., 2018). Another study revealed that the B cell-activating factor of the TNF family (BAFF) promotes IgA production and eosinophil activation, with increased presence of both naïve and effector B cell subtypes in CRSwNP (Miljkovic et al., 2018). Together, these findings underscore the indispensable role of B cells in both nasal mucosal health and the pathogenesis

Metabolic dysregulation plays a pivotal role in the pathogenesis of CRSwNP, as metabolites are known to modulate immune cell function and thereby influence inflammatory processes. Through Mendelian randomization analysis, we identified a causal relationship between the lipid metabolite 1-stearoyl-2-arachidonoyl and CRSwNP, with this metabolite exacerbating the condition. Composed of stearic acid and arachidonic acid, 1-stearoyl-2-arachidonoyl is integral to signaling pathways and



inflammatory responses, acting as a key mediator that receives upstream signals and activates downstream inflammatory cascades (Xu et al., 2022). This finding aligns with research by Hao et al., who, through transcriptomic and metabolomic studies, demonstrated that 1-stearoyl-2-arachidonoyl coordinates the release of inflammatory cytokines (Hao et al., 2023). To further explore the effects of this metabolite, we conducted cell subpopulation annotation and differential gene expression analysis based on varying metabolic levels of 1-stearoyl-2-arachidonoyl. Our results revealed that B cell subpopulations exhibiting high metabolism of this lipid are closely associated with immune response pathways, including adaptive immune responses and positive regulation of the immune system, suggesting a pro-inflammatory role in CRSwNP. Additionally, differential gene analysis indicated significant upregulation of CD27, DERL3, and TNFRSF17 in these subpopulations, highlighting their involvement in the pro-inflammatory functions driven by 1-stearoyl-2-arachidonoyl metabolism.

CD27, a cell surface molecule belonging to the tumor necrosis factor receptor (TNFR) superfamily, plays a critical role in immune responses by promoting B cell survival and antibody production (Grimsholm, 2023). Upon antigenic stimulation, CD27⁺ B cells differentiate more efficiently into plasma cells and generate

antibodies, a process facilitated by the interaction between CD27 and its ligand CD70, which provides co-stimulatory signals that enhance B cell activation and proliferation (Borst et al., 2005). Additionally, CD27 has been implicated in the differentiation of mouse B cells into memory B cells (Raman et al., 2003), and it directly drives the synthesis of IgG and IgM, both of which are essential in inflammatory processes. Notably, IgM+CD27+ B cells exhibit immunomodulatory functions and serve as a significant source of IL-10 (Sun et al., 2019), further underscoring the multifaceted role of CD27 in B cell-mediated immunity.

DERL3 (Derlin-3), a member of the Derlin family involved in protein folding and cellular stress responses, has been shown to exacerbate inflammation through the activation of NF- κ B (Geng et al., 2020). Research by Li et al. also highlights DERL3's close association with immune regulation, particularly in adaptive immune response and immune response regulation pathways (Li et al., 2020), which aligns with our findings. Similarly, TNFRSF17 (Tumor Necrosis Factor Receptor Superfamily, Member 17), also known as B-Cell Maturation Antigen (BCMA), is a TNFR superfamily member predominantly expressed on mature B cells and plasma cells. It regulates B cell survival, differentiation, and function, with BAFF mediating B cell activation through BCMA

(Saltzman et al., 2013). Furthermore, TNFRSF17/BCMA is involved in antibody production and the formation of immune memory (Sabat et al., 2023), emphasizing its significance in sustaining immune responses. Together, the upregulation of CD27, DERL3, and TNFRSF17 in B cells within CRSwNP underscores their collective contribution to the pro-inflammatory milieu and immune dysregulation characteristic of this condition.

While our integrated multi-omics approach provides robust evidence for immunometabolic dysregulation in CRSwNP, several limitations should be acknowledged. Mendelian randomization offers evidence of potential causal associations but may be affected by pleiotropy or population stratification, despite FDR correction. The metabolomics analysis used a small sample size (12 controls and 19 patients), potentially limiting generalizability due to variability in collection and metabolite stability. Public datasets for scRNA-seq (GSE196169) and bulk RNA-seq (GSE36830, GSE23552) introduce risks of batch effects and heterogeneity from different platforms or populations. Inferences linking 1-stearoyl-2-arachidonoyl to B cell functions rely on correlations, which could be influenced by unmeasured confounders. No functional experiments (e.g., in vitro validations) were performed to confirm mechanisms. Future studies with larger, multi-ethnic cohorts and experimental validations are needed to enhance these findings.

5 Conclusion

Our study underscores the critical interplay between immune and metabolic processes in the pathogenesis of CRSwNP. Notably, the metabolite 1-stearoyl-2-arachidonoyl has been shown to bind to B-cell receptors, thereby enhancing inflammatory responses. Additionally, our findings highlight the significant roles of genes such as CD27, DERL3, and TNFRSF17 in shaping the immune microenvironment, elucidating specific pathological mechanisms underlying CRSwNP. A deeper comprehension of these molecular and cellular pathways offers a robust foundation for the development of personalized therapeutic strategies, with the potential to optimize clinical management and improve patient outcomes.

Data availability statement

The metabolomic data have been uploaded to MetaboLights (accession number: MTBLS13192), available at https://www.ebi.ac.uk/metabolights/editor/MTBLS13192/descriptors. Further inquiries can be directed to the corresponding author.

Ethics statement

This study was approved by the Medical Ethics Committee of Guangzhou Red Cross Hospital (Approval No: 2024-128-01), conducted in accordance with the Declaration of Helsinki, and all participants provided written informed consent.

Author contributions

Analysis, Methodology, JW: Formal Writing - original draft, Investigation, Conceptualization. YS: Data curation, Methodology, Conceptualization, Writing - original draft, Formal Analysis. SW: Data curation, Methodology, Conceptualization, Formal Analysis, Writing - original draft. QZ: Writing - original draft, Validation, Visualization, Methodology, Investigation, Software. YL: Writing - original draft, Resources. CL: Methodology, Writing - original draft, Resources. MA: Data curation, Formal Analysis, Writing - original draft. FY: Supervision, Conceptualization, Writing - review and editing, Project administration, Funding acquisition. LC: Conceptualization, Project administration, Supervision, Writing - review and editing, Funding acquisition.

Funding

The author(s) declare that financial support was received for the research and/or publication of this article. This work was funded by the Guangzhou Science and Technology Planning Project (No. 2025A03J3381, No. 2024A03J0564, No. 202201020067) and the Guangdong Provincial Bureau of Traditional Chinese Medicine Foundation (Grant No. 20241228).

Conflict of interest

The authors declare that the research was conducted in the absence of any commercial or financial relationships that could be construed as a potential conflict of interest.

Generative AI statement

The author(s) declare that no Generative AI was used in the creation of this manuscript.

Any alternative text (alt text) provided alongside figures in this article has been generated by Frontiers with the support of artificial intelligence and reasonable efforts have been made to ensure accuracy, including review by the authors wherever possible. If you identify any issues, please contact us.

Publisher's note

All claims expressed in this article are solely those of the authors and do not necessarily represent those of their affiliated organizations, or those of the publisher, the editors and the reviewers. Any product that may be evaluated in this article, or claim that may be made by its manufacturer, is not guaranteed or endorsed by the publisher.

Supplementary material

The Supplementary Material for this article can be found online at: https://www.frontiersin.org/articles/10.3389/fphar.2025.1719897/full#supplementary-material

SUPPLEMENTARY FIGURE S1

Gene expression analysis of CRSwNP. (A) PCA before data integration. (B) PCA after data integration. (C) Heatmap of gene expression in CRSwNP group versus normal group. (D) Volcano plot of gene expression in

CRSwNP group versus normal group. **(E)** Box plot of gene expression in CRSwNP group versus normal group.

SUPPLEMENTARY FIGURE S2

Correlation analysis of differentially expressed genes in CRSwNP.

(A) Correlation analysis of differentially expressed genes across all groups.

(B) Correlation analysis of differentially expressed genes in the CRSwNP group. (C) Correlation analysis of significantly differentially expressed genes. (D) Correlation analysis of DERL3 and CD27. (E) Correlation analysis of FKBP11 and CD27.

References

Bachert, C., Bhattacharyya, N., Desrosiers, M., and Khan, A. H. (2021). Burden of disease in chronic rhinosinusitis with nasal polyps. *J. Asthma Allergy* 14, 127–134. doi:10.2147/IAA.S290424

Bai, J., and Tan, B. K. (2023). B lineage cells and IgE in allergic rhinitis and CRSwNP and the role of omalizumab treatment. *Am. J. Rhinology Allergy* 37 (2), 182–192. doi:10. 1177/19458924221147770

Bangert, C., Villazala-Merino, S., Fahrenberger, M., Krausgruber, T., Bauer, W. M., Stanek, V., et al. (2022). Comprehensive analysis of nasal polyps reveals a more pronounced type 2 transcriptomic profile of epithelial cells and mast cells in aspirin-exacerbated respiratory disease. *Front. Immunol.* 13, 850494. doi:10.3389/fimmu.2022.850494

Borst, J., Hendriks, J., and Xiao, Y. (2005). CD27 and CD70 in T cell and B cell activation. Curr. Opin. Immunol. 17 (3), 275–281. doi:10.1016/j.coi.2005.04.004

Burgess, S., Butterworth, A., and Thompson, S. G. (2013). Mendelian randomization analysis with multiple genetic variants using summarized data. *Genet. Epidemiol.* 37 (7), 658–665. doi:10.1002/gepi.21758

Chen, Y., Lu, T., Pettersson-Kymmer, U., Stewart, I. D., Butler-Laporte, G., Nakanishi, T., et al. (2023). Genomic atlas of the plasma metabolome prioritizes metabolites implicated in human diseases. *Nat. Genet.* 55 (1), 44–53. doi:10.1038/s41588-022-01270-1

Cao, P. P., Li, H. B., Wang, B. F., Wang, S. B., You, X. J., Cui, Y. H., et al. (2009). Distinct immunopathologic characteristics of various types of chronic rhinosinusitis in adult Chinese. *J. allergy Clin. Immunol.* 124 (3), 478–484.e4842. doi:10.1016/j.jaci.2009.

Eide, J. G., Wu, J., Stevens, W. W., Bai, J., Hou, S., Huang, J. H., et al. (2022). Anti-phospholipid antibodies are elevated and functionally active in chronic rhinosinusitis with nasal polyps. *Clin. Exp. Allergy* 52 (8), 954–964. doi:10.1111/cea.14120

Feldman, S., Kasjanski, R., Poposki, J., Hernandez, D., Chen, J. N., Norton, J. E., et al. (2017). Chronic airway inflammation provides a unique environment for B cell activation and antibody production. *Clin. Exp. Allergy* 47 (4), 457–466. doi:10.1111/cea.12878

Fujieda, S., Imoto, Y., Kato, Y., Ninomiya, T., Tokunaga, T., Tsutsumiuchi, T., et al. (2019). Eosinophilic chronic rhinosinusitis. *Allergol. Int.* 68 (4), 403–412. doi:10.1016/j. alit.2019.07.002

Geng, M., Xu, K., Meng, L., Xu, J., Jiang, C., Guo, Y., et al. (2020). Up-regulated DERL3 in fibroblast-like synoviocytes exacerbates inflammation of rheumatoid arthritis. *Clin. Immunol.* 220, 108579. doi:10.1016/j.clim.2020.108579

Grimsholm, O. (2023). CD27 on human memory B cells-more than just a surface marker. Clin. Exp. Immunol. 213 (2), 164–172. doi:10.1093/cei/uxac114

Guo, S., Tian, M., Fan, Y., and Zhang, X. (2023). Recent advances in mass spectrometry-based proteomics and metabolomics in chronic rhinosinusitis with nasal polyps. *Front. Immunol.* 14, 1267194. doi:10.3389/fimmu.2023.1267194

Hao, R., Xiao, H., Wang, H., Deng, P., Yue, Y., Li, J., et al. (2023). Transcriptomics integrated with metabolomics unravels the interweaving of inflammatory response and 1-stearoyl-2-arachidonoyl-sn-glycerol metabolic disorder in chronic cadmium exposure-induced hepatotoxicity. *Environ. Toxicol. Pharmacol.* 101, 104172. doi:10. 1016/j.etap.2023.104172

Hox, V., Lourijsen, E., Jordens, A., Aasbjerg, K., Agache, I., Alobid, I., et al. (2020). Benefits and harm of systemic steroids for short- and long-term use in rhinitis and rhinosinusitis: an EAACI position paper. *Clin. Transl. allergy* 10, 1. doi:10.1186/s13601-019-0303-6

Hulse, K. E., Norton, J. E., Suh, L., Zhong, Q., Mahdavinia, M., Simon, P., et al. (2013). Chronic rhinosinusitis with nasal polyps is characterized by B-cell inflammation and EBV-induced protein 2 expression. *J. Allergy Clin. Immunol* 131 (4), 1075–1083.e10837. doi:10.1016/j.jaci.2013.01.043

Ishwaran, H., and Kogalur, U. B. (2010). Consistency of random survival forests. Statistics Probab. Lett. 80 (13-14), 1056-1064. doi:10.1016/j.spl.2010.02.020

Jin, Y., Wang, Z., He, D., Zhu, Y., Chen, X., and Cao, K. (2021). Identification of novel subtypes based on ssGSEA in immune-related prognostic signature for tongue squamous cell carcinoma. *Cancer Med.* 10 (23), 8693–8707. doi:10.1002/cam4.4341

Kanehisa, M., Furumichi, M., Sato, Y., Kawashima, M., and Ishiguro-Watanabe, M. (2023). KEGG for taxonomy-based analysis of pathways and genomes. *Nucleic Acids Res.* 51 (D1), D587–D592. doi:10.1093/nar/gkac963

Kim, N., Ramon, S., Thatcher, T. H., Woeller, C. F., Sime, P. J., and Phipps, R. P. (2015). Specialized proresolving mediators (SPMs) inhibit human B-cell IgE production. *Eur. J. Immunol.* 46 (1), 81–91. doi:10.1002/eji.201545673

Laidlaw, T. M., Mullol, J., Woessner, K. M., Amin, N., and Mannent, L. P. (2021). Chronic rhinosinusitis with nasal polyps and asthma. *J. Allergy Clin. Immunol. Pract.* 9 (3), 1133–1141. doi:10.1016/j.jaip.2020.09.063

Langfelder, P., and Horvath, S. (2008). WGCNA: an R package for weighted correlation network analysis. *BMC Bioinforma*. 9, 559. doi:10.1186/1471-2105-9-559

Li, Y., Liu, H., Chen, H., Shao, J., Su, F., Zhang, S., et al. (2020). DERL3 functions as a tumor suppressor in gastric cancer. *Comput. Biol. Chem.* 84, 107172. doi:10.1016/j.compbiolchem.2019.107172

Ma, Y., Wei, Y., Liu, X., Dang, H., Zou, H., Tian, P., et al. (2021). Metabolomics analysis of metabolic patterns in chronic rhinosinusitis with nasal polyps. *Allergy* 77 (2), 653–656. doi:10.1111/all.15179

Miljkovic, D., Psaltis, A., Wormald, P.-J., and Vreugde, S. (2018). Naive and effector B-cell subtypes are increased in chronic rhinosinusitis with polyps. *Am. J. Rhinology Allergy* 32 (1), 3–6. doi:10.2500/ajra.2018.32.4496

Miyata, J., Fukunaga, K., Kawashima, Y., Watanabe, T., Saitoh, A., Hirosaki, T., et al. (2019). Dysregulated fatty acid metabolism in nasal polyp-derived eosinophils from patients with chronic rhinosinusitis. *Allergy* 74 (6), 1113–1124. doi:10.1111/all.13726

Nakayama, T., and Haruna, S.-I. (2023). A review of current biomarkers in chronic rhinosinusitis with or without nasal polyps. *Expert Rev. Clin. Immunol.* 19 (8), 883–892. doi:10.1080/1744666X.2023.2200164

Newman, A. M., Liu, C. L., Green, M. R., Gentles, A. J., Feng, W., Xu, Y., et al. (2015). Robust enumeration of cell subsets from tissue expression profiles. *Nat. Methods* 12 (5), 453–457. doi:10.1038/nmeth.3337

Orru, V., Steri, M., Sidore, C., Marongiu, M., Serra, V., Olla, S., et al. (2020). Complex genetic signatures in immune cells underlie autoimmunity and inform therapy. *Nat. Genet.* 52 (10), 1036–1045. doi:10.1038/s41588-020-0684-4

Plager, D. A., Kahl, J. C., Asmann, Y. W., Nilson, A. E., Pallanch, J. F., Friedman, O., et al. (2010). Gene transcription changes in asthmatic chronic rhinosinusitis with nasal polyps and comparison to those in atopic dermatitis. *PLoS One* 5 (7), e11450. doi:10. 1371/journal.pone.0011450

Powers, R. K., Goodspeed, A., Pielke-Lombardo, H., Tan, A. C., and Costello, J. C. (2018). GSEA-InContext: identifying novel and common patterns in expression experiments. *Bioinformatics* 34 (13), i555–i564. doi:10.1093/bioinformatics/bty271

Raman, V. S., Akondy, R. S., Rath, S., Bal, V., and George, A. (2003). Ligation of CD27 on B cells in vivo during primary immunization enhances commitment to memory B cell responses. *J. Immunol.* 171 (11), 5876–5881. doi:10.4049/jimmunol.171.

Ritchie, M. E., Phipson, B., Wu, D., Hu, Y., Law, C. W., Shi, W., et al. (2015). Limma powers differential expression analyses for RNA-sequencing and microarray studies. *Nucleic Acids Res.* 43 (7), e47. doi:10.1093/nar/gkv007

Ryu, G., Kim, D.-K., Dhong, H.-J., Eun, K. M., Lee, K. E., Kong, I. G., et al. (2019). Immunological characteristics in refractory chronic rhinosinusitis with nasal polyps undergoing revision surgeries. *Allergy, Asthma Immunol. Res.* 11 (5), 664–676. doi:10. 4168/aair.2019.11.5.664

Sabat, R., Šimaitė, D., Gudjonsson, J. E., Brembach, T.-C., Witte, K., Krause, T., et al. (2023). Neutrophilic granulocyte-derived B-cell activating factor supports B cells in skin lesions in hidradenitis suppurativa. *J. Allergy Clin. Immunol.* 151 (4), 1015–1026. doi:10. 1016/j.jaci.2022.10.034

Saltzman, J. W., Battaglino, R. A., Salles, L., Jha, P., Sudhakar, S., Garshick, E., et al. (2013). B-Cell maturation antigen, A proliferation-inducing ligand, and B-Cell activating factor are candidate mediators of spinal cord injury-induced autoimmunity. *J. Neurotrauma* 30 (6), 434–440. doi:10.1089/neu.2012.2501

Schleimer, R. P. (2017). Immunopathogenesis of chronic rhinosinusitis and nasal polyposis. *Annu. Rev. Pathology Mech. Dis.* 12 (1), 331–357. doi:10.1146/annurev-pathol-052016-100401

Stevens, W. W., Ocampo, C. J., Berdnikovs, S., Sakashita, M., Mahdavinia, M., Suh, L., et al. (2015). Cytokines in chronic rhinosinusitis. Role in eosinophilia and aspirinexacerbated respiratory disease. *Am. J. Respir. Crit. Care Med.* 192 (6), 682–694. doi:10.1164/rccm.201412-2278OC

Stuart, T., Butler, A., Hoffman, P., Hafemeister, C., Papalexi, E., Mauck, W. M., et al. (2019). Comprehensive integration of single-cell data. *Cell* 177 (7), 1888–1902.e21. doi:10.1016/j.cell.2019.05.031

Sun, H., Zhang, Y., Song, W., Yin, L., Wang, G., Yu, D., et al. (2019). IgM+CD27+B cells possessed regulatory function and represented the main source of B cell-derived IL-10 in the synovial fluid of osteoarthritis patients. *Hum. Immunol.* 80 (4), 263–269. doi:10.1016/j.humimm.2019.02.007

Tan, B. K., Peters, A. T., Schleimer, R. P., and Hulse, K. E. (2018). Pathogenic and protective roles of B cells and antibodies in patients with chronic rhinosinusitis. *J. Allergy Clin. Immunol.* 141 (5), 1553–1560. doi:10.1016/j.jaci.2018.03.002

Veloso-Teles, R., Cerejeira, R., Roque-Farinha, R., and Cv, B. (2019). Systemic immune profile in patients with CRSwNP. *Ear, Nose Throat J.* 100 (5_Suppl. l), 554S–561S. doi:10.1177/0145561319893163

Vickery, T. W., Armstrong, M., Kofonow, J. M., Robertson, C. E., Kroehl, M. E., Reisdorph, N. A., et al. (2021). Altered tissue specialized pro-resolving mediators in chronic rhinosinusitis. *Prostagl. Leukot. Essent. Fat. Acids* 164, 102218. doi:10.1016/j.plefa.2020.102218

Wilkerson, M. D., and Hayes, D. N. (2010). Consensus ClusterPlus: a class discovery tool with confidence assessments and item tracking. *Bioinformatics* 26 (12), 1572–1573. doi:10.1093/bioinformatics/btq170 Xu, Q., Wu, C., Zhu, Q., Gao, R., Lu, J., Valles-Colomer, M., et al. (2022). Metagenomic and metabolomic remodeling in nonagenarians and centenarians and its association with genetic and socioeconomic factors. *Nat. Aging* 2 (5), 438–452. doi:10.1038/s43587-022-00193-0

Xu, H., Jiang, L., Qin, L., Shi, P., Xu, P., and Liu, C. (2024). Single-cell transcriptome analysis reveals intratumoral heterogeneity in lung adenocarcinoma. *Environ. Toxicol.* 39 (3), 1847–1857. doi:10.1002/tox.24048

Zhai, G.-T., Wang, H., Li, J.-X., Cao, P.-P., Jiang, W.-X., Song, J., et al. (2018). IgD-activated mast cells induce IgE synthesis in B cells in nasal polyps. *J. Allergy Clin. Immunol.* 142 (5), 1489–1499.e23. doi:10.1016/j.jaci.2018.07.025

Zhang, Y., Liu, T., Hu, X., Wang, M., Wang, J., Zou, B., et al. (2021). CellCall: integrating paired ligand-receptor and transcription factor activities for cell-cell communication. *Nucleic Acids Res.* 49 (15), 8520–8534. doi:10.1093/nar/gkab638

Zhang, F., Xu, Z., He, X., Sun, Y., Zhao, C., Zhang, J., et al. (2022). Increased B cell-activating factor expression is associated with postoperative recurrence of chronic rhinosinusitis with nasal polyps. *Mediat. Inflamm.* 2022, 7338692–11. doi:10.1155/2022/7338692

Zheng, G. X., Terry, J. M., Belgrader, P., Ryvkin, P., Bent, Z. W., Wilson, R., et al. (2017). Massively parallel digital transcriptional profiling of single cells. *Nat. Commun.* 8, 14049. doi:10.1038/ncomms14049

Zhou, Y., Zhou, B., Pache, L., Chang, M., Khodabakhshi, A. H., Tanaseichuk, O., et al. (2019). Metascape provides a biologist-oriented resource for the analysis of systems-level datasets. *Nat. Commun.* 10 (1), 1523. doi:10.1038/s41467-019-09234-6

Zhu, Z., Zheng, Z., Zhang, F., Wu, Y., Trzaskowski, M., Maier, R., et al. (2018). Causal associations between risk factors and common diseases inferred from GWAS summary data. *Nat. Commun.* 9 (1), 224. doi:10.1038/s41467-017-02317-2

Zhu, Y., Sun, X., Tan, S., Luo, C., Zhou, J., Zhang, S., et al. (2022). M2 macrophagerelated gene signature in chronic rhinosinusitis with nasal polyps. *Front. Immunol.* 13, 1047930. doi:10.3389/fimmu.2022.1047930